



ELSEVIER

9 October 2000



PHYSICS LETTERS A

Physics Letters A 275 (2000) 173–181

www.elsevier.nl/locate/pla

Deflection of quantum particles by impenetrable boundary

V.V. Dodonov ¹, M.A. Andreata

Departamento de Física, Universidade Federal de São Carlos, Via Washington Luiz km 235, 13565-905 São Carlos, SP, Brazil

Received 9 August 2000; accepted 17 August 2000

Communicated by V.M. Agranovich

Abstract

The evolution of quantum packets in the presence of an impenetrable boundary is studied. Due to an effective ‘quantum repulsive force’, the mean value of the momentum in the direction perpendicular to the boundary gradually changes in time at the expense of the energy of quantum fluctuations, and the packet becomes significantly narrower than it would be in the free space under the same initial conditions. For zero initial mean transverse velocity, the asymptotical value of the transverse momentum depends only on the initial form of the packet, being *independent* of its initial position (provided this position is much greater than the initial transverse width of the packet). As a consequence, narrow beams of ultracold particles (e.g., atoms with velocities about 1 m/s and the initial transverse uncertainty in position about 0.01 μm) directed along an impenetrable surface will be deflected to observable angles due to the quantum (wave) nature of particles. The possibilities of the experimental verification of the effect are discussed. The conclusion on the inelasticity of collisions between ultracold particles due to the transformations of the shapes of their wave functions is made. © 2000 Elsevier Science B.V. All rights reserved.

PACS: 03.65.Bz; 03.75.-b

Keywords: Quantum packets; Impenetrable boundary; Ultracold particles; Matter waves

1. Introduction

The propagation of quantum packets in *free space* is one of the most known problems of quantum mechanics, discussed in practically all textbooks. It is well known that initially localized packets spread unlimitedly over the space with the course of time. Moreover, the mean position $\langle x \rangle \equiv \int \psi^* x \psi dx$ and

the mean momentum $\langle p \rangle \equiv -i\hbar \int \psi^* (\partial\psi/\partial x) dx$ remain completely independent of the (co)variances, $\sigma_x \equiv \langle x^2 \rangle - \langle x \rangle^2$, $\sigma_p \equiv \langle p^2 \rangle - \langle p \rangle^2$, $\sigma_{px} = \sigma_{xp} \equiv \frac{1}{2} \langle xp + px \rangle - \langle x \rangle \langle p \rangle$, which are related to the *shape* of the packet. The (Ehrenfest) equations of motion for these average values are the same as in the classical case:

$$d\langle x \rangle/dt = \langle p \rangle/m, \quad d\langle p \rangle/dt = 0, \quad (1)$$

$$\dot{\sigma}_x = \frac{2}{m} \sigma_{xp}, \quad \dot{\sigma}_{xp} = \frac{1}{m} \sigma_p, \quad \dot{\sigma}_p = 0, \quad (2)$$

where m is the particle mass.

E-mail address: vdodonov@df.ufscar.br (V.V. Dodonov).

¹ On leave from Lebedev Physics Institute and Moscow Institute of Physics and Technology, Russia.

The situation changes, if a particle moves in some external potential. Excluding the case of *quadratic Hamiltonians*, studied in detail, e.g., in [1], the evolution of the first-order mean values depends on the higher-order moments, and instead of simple independent equations like (1) and (2) one has to solve, generally speaking, an infinite set of coupled equations. Various kinds of *semiclassical* wave packets were considered in the frameworks of different approaches, e.g., in [2–7].

The limiting case of an abrupt infinitely high potential is equivalent to the problem of motion in the *semispace* $x > 0$, when the presence of an impenetrable boundary imposes the boundary condition for the wave function

$$\psi(0, t) \equiv 0. \quad (3)$$

This problem was considered in several studies, devoted, in particular, to calculating exact or quasiclassical propagators in the presence of additional potentials and for various geometrical configurations and boundary conditions [8–12]. Another direction of research is connected with theoretical and experimental studies of ultracold particles bouncing on an impenetrable boundary due to the gravitational force or its equivalents (such systems are usually called as ‘gravitational traps’ in the neutron physics [13,14] and ‘gravitational cavities’ in the atomic physics [15–19]).

We would like to draw an attention to the problem of influence of an ideal boundary on the motion of ultraslow quantum particles, whose initial mean momentum $\langle p(0) \rangle$ is less than the mean squared value of the quantum fluctuations $\sqrt{\sigma_p(0)}$ (an opposite case of $\langle p(0) \rangle \gg \sqrt{\sigma_p(0)}$ was studied recently in [20]). Despite its mathematical simplicity, this problem could be interesting from the point of view of possible *experiments* with ultraslow particles, emphasizing their quantum (wave) nature. Namely, throwing an ultracold atom (with the velocity of the order of 1 m/s or less) in the direction parallel to an impenetrable boundary, one could observe that the atom would be *deflected* from the boundary. What is the most impressive, it is the fact that the deflection angle (which can be, in principle, arbitrarily large, depending on the initial velocity and the initial transverse uncertainty of the particle position) *does not*

depend on the initial distance from the boundary. Therefore, this is a pure quantum effect, which could be performed on the basis of the available skill of experiments with ultracold particles.

2. Evolution of packets and mean values in the presence of an impenetrable boundary

In the case involved, the integrals defining the mean values have the lower limit $x = 0$. This fact does not affect the first Ehrenfest equation, $d\langle x \rangle/dt = \langle p \rangle/m$. To calculate the time derivative of $\langle p \rangle$, we replace the time derivative of the wave function by its second-order space derivative according to the Schrödinger equation

$$\partial\psi/\partial t = (i\hbar/2m)\partial^2\psi/\partial x^2 \quad (4)$$

and apply the integration by parts. Taking into account the boundary condition (3), we obtain the modified second Ehrenfest equation:

$$d\langle p \rangle/dt = \frac{\hbar^2}{2m} \left| \frac{\partial\psi}{\partial x}(x=0) \right|^2 \equiv F_r(t), \quad (5)$$

where $F_r(t)$ can be interpreted as an effective ‘quantum repulsive force’. This force is always positive, so it causes the ‘center of mass’ of the quantum packet to move far from the boundary. The noncentralized second-order moments, $\langle x^2 \rangle$, $\langle xp + px \rangle$, and $\langle p^2 \rangle$, obey the same equations as in the free space case. Therefore the variances are no more independent of the first-order mean values, since the second and the third equations in (2) take the form

$$\dot{\sigma}_{xp} = \frac{1}{m}\sigma_p - F_r(t)\langle x \rangle, \quad \dot{\sigma}_p = -2F_r(t)\langle p \rangle. \quad (6)$$

In this Letter we confine ourselves to studying the evolution of the packets in the special case of zero initial mean momentum: $\langle p(0) \rangle = 0$. Then the quantities $F_r(t)$, $\langle x \rangle$ and $\langle p \rangle$ are always nonnegative, and all three (co)variances turn out less than they would be in the case of the free space evolution (for the same initial conditions). This means that the presence of the boundary makes the packet narrower, both with respect to the momentum and coordinate.

The solutions to the Schrödinger Eq. (4) satisfying the boundary condition (3) can be easily obtained from the solutions in the full space $\psi_f(x,t)$ [21]:

$$\psi(x,t) = \psi_f(x,t) - \psi_f(-x,t). \quad (7)$$

We confine ourselves to the family of solutions originating from the well known *Gaussian packets* in the free space. We use the parametrization of such packets proposed in [22] for the problem of quantum oscillator with a time-dependent frequency:

$$\begin{aligned} \psi_\alpha^{(f)}(x,t) = & \left[\frac{m}{\pi \hbar \varepsilon^2(t)} \right]^{1/4} \exp \left[\frac{im\dot{\varepsilon}}{2\hbar\varepsilon} x^2 \right. \\ & \left. + i\sqrt{2m/\hbar} \frac{\alpha x}{\varepsilon} + \frac{\varepsilon^* \alpha^2}{2\varepsilon} - \frac{1}{2} |\alpha|^2 \right]. \end{aligned} \quad (8)$$

The time dependence is ‘hidden’ in the complex function $\varepsilon(t)$, which is an arbitrary solution to the classical equation

$$\ddot{\varepsilon} + \omega^2(t) \varepsilon = 0, \quad (9)$$

satisfying the normalization condition

$$\dot{\varepsilon} \varepsilon^* - \dot{\varepsilon}^* \varepsilon = 2i. \quad (10)$$

The case of a free motion corresponds to $\omega \equiv 0$ in Eq. (9), i.e., to the linear dependence

$$\varepsilon(t) = a + ibt, \quad \text{Re}(ba^*) = 1. \quad (11)$$

Function (8) can be considered as a *coherent state*, since it is the eigenfunction of the nonhermitian time-dependent annihilation operator integral of motion [22]:

$$\hat{a} \psi_\alpha^{(f)} = \alpha \psi_\alpha^{(f)}, \quad \hat{a} = \frac{\varepsilon \hat{p} - m \dot{\varepsilon} \hat{x}}{\sqrt{2m\hbar}}, \quad [\hat{a}, \hat{a}^\dagger] = 1. \quad (12)$$

The general form (8) can be used, besides the cases of the oscillator and the free motion, also for the ‘upside-down oscillator’ (when $\omega^2 < 0$) and (after some modifications) for the most general one-dimensional quadratic Hamiltonians: see, e.g., [23].

Using the recipe (7) we obtain the following normalized solution in the semi-space $x > 0$:

$$\begin{aligned} \psi_\alpha(x,t) = & 2\mathcal{N}(|\alpha|) \left[\frac{m}{\pi \hbar \varepsilon^2(t)} \right]^{1/4} \\ & \times \exp \left[\frac{im\dot{\varepsilon}}{2\hbar\varepsilon} x^2 + \frac{\varepsilon^* \alpha^2}{2\varepsilon} - \frac{1}{2} |\alpha|^2 \right] \\ & \times \sin \left(\sqrt{2m/\hbar} \frac{\alpha x}{\varepsilon} \right), \\ \mathcal{N}(|\alpha|) = & [1 - \exp(-2|\alpha|^2)]^{-1/2}. \end{aligned} \quad (13)$$

The solution (13) was found for the first time in [24] under the name *odd coherent state*. It is the eigenfunction of the operator \hat{a}^2 defined in (12), with the eigenvalue α^2 .

We assume, without any loss of generality (since any change of constant phase of the complex number ε can be compensated by the change of the phase of the complex number α), that constant number b in formula (11) is real and positive. Then $a = (1 + i\gamma)/b$, where a constant real number γ is responsible for the initial nonzero covariance $\sigma_{p,x}(0)$. In this Letter, we do not analyse the most general situation, confining ourselves to the most simple (but quite interesting) case of zero initial covariance and mean momentum, $\sigma_{p,x}(0) = \langle p(0) \rangle = 0$. These conditions are satisfied for the following specific choice of the complex function $\varepsilon(t)$ and the complex coherent parameter α :

$$\varepsilon(t) = b^{-1} + ibt, \quad \alpha = -i\beta, \quad b, \beta > 0. \quad (14)$$

Besides, we assume that the initial mean value of the coordinate is much greater than the initial packet width. This condition is equivalent (see below) to $\beta \gg 1$, therefore the factor $\mathcal{N}(|\alpha|)$ can be replaced by unity with the accuracy of the order of $\exp(-2\beta^2)$. Under the assumptions made, the initial coordinate distribution $\mathcal{P}_x(x,0) = |\psi(x,0)|^2$ is very close to the Gaussian,

$$\mathcal{P}_x(x,0) \approx (\pi s^2)^{-1/2} \exp \left[-(x - x_c)^2 / s^2 \right], \quad (15)$$

where the initial distance between the boundary and the center of the packet x_c , and the packet width s are given by the expressions

$$x_c = \beta\sqrt{2\hbar/(mb^2)}, \quad s = \sqrt{\hbar/(mb^2)}. \quad (16)$$

Consequently, $x_c/s = \beta\sqrt{2}$.

The quantity $\langle p^2 \rangle$ does not depend on time:

$$\langle p^2 \rangle = \frac{1}{2}m\hbar b^2 = \hbar^2/(2ms^2) \quad (17)$$

(hereafter we neglect small corrections of the order of $\exp(-2\beta^2)$ in all the expressions). Two other second-order moments depend on time as

$$\begin{aligned} \langle x^2 \rangle &= \frac{\hbar}{2mb^2}(1 + 4\beta^2 + b^4t^2) \\ &= \frac{s^2}{2} + x_c^2 + \frac{(\hbar t)^2}{2(ms)^2}, \end{aligned} \quad (18)$$

$$\langle px + xp \rangle = \hbar b^2 t. \quad (19)$$

We see that for $t > 0$, the *correlation coefficient* $r = \sigma_{px}/\sqrt{\sigma_p\sigma_x}$ is different from zero. The states with $r \neq 0$ were named *correlated states* in [25] and (in the special case of Gaussian packets in the free space) ‘contractive states’ in [26–28]. For other studies on such states see, e.g., [1,29–31].

It is convenient to introduce the dimensionless variables

$$\tilde{x} = \frac{x}{x_c}, \quad \tilde{p} = \frac{p}{b\sqrt{m\hbar}} = \frac{ps}{\hbar}, \quad \tau = \frac{b^2}{\beta}t = \frac{\hbar\sqrt{2}}{msx_c}t. \quad (20)$$

Then the first-order average values of the momentum and coordinate in state (13) can be expressed as

$$\langle \tilde{p}(\tau) \rangle = \sqrt{2} \beta \operatorname{erfi}\left(\frac{\sqrt{2} \beta^2 \tau}{\sqrt{1 + \beta^2 \tau^2}}\right) e^{-2\beta^2}, \quad (21)$$

$$\begin{aligned} \langle \tilde{x}(\tau) \rangle &= \operatorname{erf}\left(\frac{\sqrt{2} \beta}{\sqrt{1 + \beta^2 \tau^2}}\right) \\ &+ \beta\tau \operatorname{erfi}\left(\frac{\sqrt{2} \beta^2 \tau}{\sqrt{1 + \beta^2 \tau^2}}\right) e^{-2\beta^2}. \end{aligned} \quad (22)$$

The error function $\operatorname{erf}(x)$ and its modification $\operatorname{erfi}(x)$ are defined as follows,

$$\operatorname{erf}(x) = \frac{2}{\sqrt{\pi}} \int_0^x e^{-t^2} dt, \quad \operatorname{erfi}(x) = \frac{2}{\sqrt{\pi}} \int_0^x e^{t^2} dt.$$

The wave packet preserves its initial form (15) only for rather short time, until $b^2t \ll 1$ (i.e., $\tau \ll \beta^{-1}$). Then it begins to spread with almost constant velocity $\hbar/(ms\sqrt{2})$ (see Eq. (18)). For $\beta\tau \gg 1$, using the asymptotical formula [32]

$$\operatorname{erfi}(x \gg 1) \approx (\sqrt{\pi}x)^{-1} e^{x^2}, \quad (23)$$

we have

$$\langle \tilde{p}(\tau) \rangle = \pi^{-1/2} \exp(-2/\tau^2), \quad (24)$$

$$\langle \tilde{x}(\tau) \rangle = \operatorname{erf}(1/\tau) + \frac{\tau}{\sqrt{2\pi}} \exp(-2/\tau^2). \quad (25)$$

The dimensionless ‘quantum repulsive force’ is given by

$$\begin{aligned} \tilde{F}_r &= \frac{d\langle \tilde{p} \rangle}{d\tau} = \frac{4\beta^3/\sqrt{\pi}}{(1 + \beta^2\tau^2)^{3/2}} \exp\left(-\frac{2\beta^2}{1 + \beta^2\tau^2}\right) \\ &= 4(\tau^3\sqrt{\pi})^{-1} \exp(-2/\tau^2), \end{aligned} \quad (26)$$

where the last expression holds for $\beta\tau \gg 1$. We see that the mean values and the ‘quantum force’ exhibit universal (independent of β) behaviours for $\tau \gg \beta^{-1}$. The exponential functions in Eqs. (24)–(26) can be replaced approximately by 1 if $\tau > 5$. Then the average momentum assumes practically constant asymptotical value, which *does not depend* on β :

$$\langle p_\infty \rangle = b\sqrt{m\hbar/\pi} = \hbar/(s\sqrt{\pi}). \quad (27)$$

Consequently, $\langle p_\infty \rangle/\sqrt{\langle p^2 \rangle} = \sqrt{2/\pi} \approx 0.8$, i.e., 64% of the energy of quantum fluctuations are transformed ultimately into the energy of the center of the packet due to the presence of the wall. The final width of the packet in the momentum space is $\sqrt{1 - 2/\pi} \approx 0.6$ of the initial one. The variance σ_x is no more independent of the mean position $\langle x \rangle$. Asymptotically, for $\tau \gg 1$, we have $\sqrt{\sigma_x}/\langle x \rangle \rightarrow \sqrt{\pi/2 - 1} \approx 0.75$. The plots of $\langle \tilde{x}(\tau) \rangle$, $\langle \tilde{p}(\tau) \rangle$,

and $\tilde{F}_r(\tau)$ are given in Fig. 1. They show that the particle begins to ‘feel’ the presence of the wall when $\tau > 0.5$. This value agrees, by the order of magnitude, with the time necessary for a quantum packet to spread from its initial dimension s to the value x_c : see Eq. (18). (Note that the classical particle, for which formally $\hbar = 0$, would never ‘know’ about the boundary.)

The probability density in the coordinate space, $\mathcal{P}_x = |\psi(x)|^2$, can be expressed as follows (in the dimensionless variables),

$$\mathcal{P}_x(\tilde{x}, \tau) = \sqrt{\frac{32\beta^2}{\pi(1 + \beta^2\tau^2)}} \exp\left[-\frac{2\beta^2(1 + \tilde{x}^2)}{1 + \beta^2\tau^2}\right] \times \left[\sinh^2\left(\frac{2\beta^2\tilde{x}}{1 + \beta^2\tau^2}\right) + \sin^2\left(\frac{2\beta^3\tau\tilde{x}}{1 + \beta^2\tau^2}\right) \right]. \quad (28)$$

For $\beta\tau \gg 1$ we have

$$\mathcal{P}_x(\tilde{x}, \tau \gg \beta^{-1}) = \sqrt{\frac{32}{\pi\tau^2}} \exp\left[-\frac{2}{\tau^2}(1 + \tilde{x}^2)\right] \times \left[\sinh^2\left(\frac{2\tilde{x}}{\tau^2}\right) + \sin^2\left(\frac{2\beta\tilde{x}}{\tau}\right) \right]. \quad (29)$$

For small values of τ (actually, for $\tau < 1/2$, when the main part of the packet did not reach the bound-

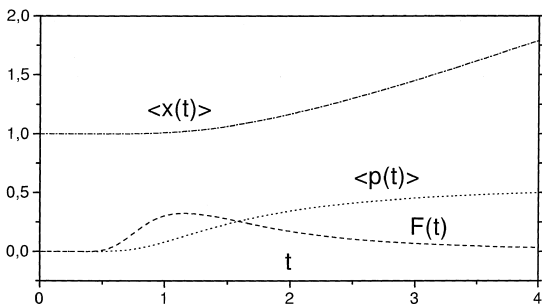


Fig. 1. Evolution of dimensionless mean values of the coordinate and momentum defined in Eq. (20) (tildes are omitted), and the dimensionless ‘quantum repulsive force’ (26), versus the dimensionless time $\tau \equiv t$, for $\beta = 10^4$.

ary and the ‘quantum force’ is practically zero), the oscillating \sin^2 term in (29) is unessential, and the probability density is given by the smooth Gaussian curve. For larger values of τ , this curve spreads into a wide strip, filled in with rapidly oscillating function $\sin^2(2\beta\tilde{x}/\tau)$. The space period of these oscillations is of the order of the initial packet width: $\Delta x = \pi s\tau/\sqrt{2}$, therefore in the case $\beta \gg 1$ the plot looks like some dark region confined with two envelopes, given by Eq. (29) with $\sin^2(2\beta\tilde{x}/\tau)$ replaced by 1 and 0, respectively. Typical examples of the coordinate distribution are shown in Fig. 2, where for $\tau = 3$ we plot only the maximal and minimal values of the rapidly oscillating probability density, and its mean value averaged over oscillations. Of course, $\mathcal{P}_x(0) = 0$, but already at $\tilde{x} \approx \pi\tau/(4\beta)$, $\mathcal{P}_x(\tilde{x})$ assumes the maximal value of the order of $3\tau^{-1}\exp(-2/\tau^2)$. The time dependence of the probability of detecting the particle to the left from the initial mean value position, $W = \int_0^1 \mathcal{P}_x(\tilde{x}) d\tilde{x}$, is also shown in Fig. 2.

The momentum distribution

$$\mathcal{P}_p(p) = \frac{1}{2\pi\hbar} \left| \int_0^\infty \psi(x) \exp(-ipx/\hbar) dx \right|^2$$

has the following form (in the dimensionless variables):

$$\mathcal{P}_p(\tilde{p}, \tau) = (16\pi)^{-1/2} \exp(-\tilde{p}^2) \left| \exp(-i\beta\tilde{p}\sqrt{2}) \times \operatorname{erfc}\left(\frac{i\tilde{p}}{\sqrt{2}}\sqrt{1+i\beta\tau} - \frac{\beta}{\sqrt{1+i\beta\tau}}\right) \times \exp(i\beta\tilde{p}\sqrt{2}) \operatorname{erfc}\left(\frac{i\tilde{p}}{\sqrt{2}}\sqrt{1+i\beta\tau} + \frac{\beta}{\sqrt{1+i\beta\tau}}\right) \right|^2, \quad (30)$$

where the complementary error function is defined as

$$\operatorname{erfc}(x) = \frac{2}{\sqrt{\pi}} \int_x^\infty e^{-t^2} dt.$$

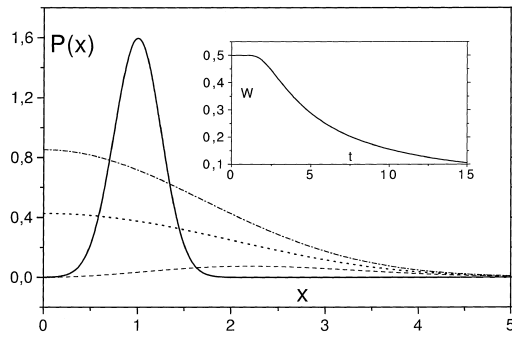


Fig. 2. The coordinate probability density versus the dimensionless coordinate $x \equiv \tilde{x}$ for $\beta = 10^4$. Solid curve – a spreaded Gaussian distribution for the dimensionless time $\tau = 0.5$. Broken curves correspond to $\tau = 3$: lower dashed curve – minimal values of the rapidly oscillating probability (29); upper dashed-dotted curve – maximal values of the rapidly oscillating probability (29); middle dotted curve – probability distribution (29) averaged over fast oscillations. In the insertion we show the dependence of the probability W of detecting the particle between the wall and the mean initial position (i.e., in the interval $0 < \tilde{x} < 1$) versus the dimensionless time $\tau \equiv t$, also for $\beta = 10^4$.

At $t = 0$, the real part of the argument of the first erfc-function in (30) is close to $-\infty$ for $\beta \gg 1$, so the value of this function is close to $\text{erfc}(-\infty) = 2$. At the same time, the value of the second term is close to $\text{erfc}(+\infty) = 0$. Thus we have a symmetrical initial distribution $\mathcal{P}_p(\tilde{p}, 0) = \pi^{-1/2} \exp(-\tilde{p}^2)$. On the contrary, for $\tau \gg 1$ (and fixed β) the second terms in the arguments of the erfc-functions become negligible. The *real parts* of both erfc-functions become close to $-\tilde{p}\sqrt{\beta\tau}/4$, resulting in the strong asymmetry for $\tau \gg 1$. If $p < 0$, then the real parts of both erfc-functions are large and *positive*, so these functions turn into zero. But if $p > 0$, then both functions are close to 2. As a result, the asymptotical distribution at $\tau \rightarrow \infty$ is different from zero only for $p > 0$, and it exhibits strong oscillations:

$$\mathcal{P}_p(\tilde{p}, \infty) = 4\mathcal{P}_p(\tilde{p}, 0) \sin^2(\beta\tilde{p}\sqrt{2}), \quad \tilde{p} > 0. \quad (31)$$

The period of oscillations is proportional to the ratio of the initial packet space width to the initial mean distance from the boundary. In Fig. 3 we show the plots of the maximal and minimal values of $\mathcal{P}_p(\tilde{p}, \tau)$ for $\tau = 6$.

The phenomenon can be interpreted as follows: partial waves (forming the total wave packet repre-

sented the quantum particle) with negative wave numbers are reflected from the boundary, becoming the waves with positive wave numbers. Eventually, as $t \rightarrow \infty$, all negative components are transformed to the positive ones. The oscillating structure of the asymptotical distribution can be explained by the interference between the waves which were outgoing from the beginning and those which have reversed their direction after passing the distance x_c (this is especially clear, if one takes into account that the phase $\beta\tilde{p}\sqrt{2}$ of the sine-function in (31) can be rewritten, due to (16) and (20), as px_c/\hbar). Therefore, some waves disappear completely, whereas some others can be significantly amplified (up to 4 times in energy). However, if the precision of a measuring apparatus is not sufficient to resolve the oscillations, one can use very simple average asymptotical distribution $\overline{\mathcal{P}}_p(\tilde{p}, \infty) = 2\mathcal{P}_p(\tilde{p}, 0)$ (for $\tilde{p} > 0$).

Now it is easy to understand what can happen in the case of a nonideal boundary. If the potential energy increases to infinity not abruptly, but continuously, then the *averaged* asymptotical momentum distribution will be $2\mathcal{P}_p(\tilde{p}, 0)$ for any initial distribution (since all initial partial plane waves with $p < 0$ will be finally reflected from the boundary),

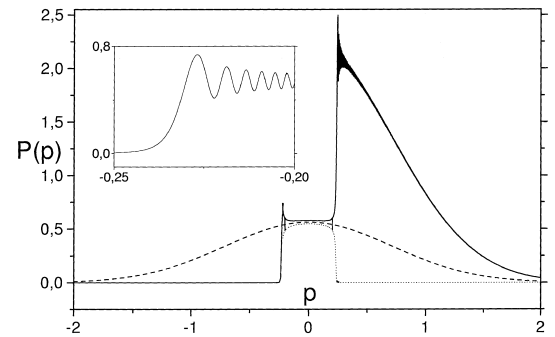


Fig. 3. The momentum distribution versus the dimensionless momentum $p \equiv \tilde{p}$ for $\beta = 10^4$ and $\tau = 6$. Upper solid curve – maximal values of the rapidly oscillating probability (30); for $p > 0.5$ the ordinates of this curve are exactly 4 times higher than the ordinates of the initial Gaussian distribution given by the middle dashed curve. Lower dotted curve – minimal values of the rapidly oscillating probability (30); they are different from zero only in the interval $|p| < 0.25$, where the amplitudes of oscillations are relatively small. In the insertion we show the details of the behaviour of function $P(p)$ in the interval $-0.25 < p < -0.20$.

although the time of establishing this distribution, as well as the details of the oscillating structure, will depend on the form of the potential. For the particle moving initially toward the boundary, the center of the initial momentum distribution is shifted to the left from point $p = 0$. In this case, the difference between the asymptotical mean value of the momentum and its initial absolute value, $\langle p(\infty) \rangle - |\langle p(0) \rangle|$, will be less than in the case of $\langle p(0) \rangle = 0$, going to zero when $\langle p(0) \rangle$ is much greater than the width of the momentum distribution, $\delta p \sim \hbar/s$ (this case was analyzed in [20]). If the potential barrier has a finite height, then some partial plane waves will not be reflected completely, and the final distribution, being deformed and asymmetrical, will have some nonzero part in the region $p < 0$, which also diminishes the asymptotical value $\langle p(\infty) \rangle$.

3. ‘Quantum deflection’ of ultracold particles

The results of the preceding section seem almost obvious from the point of view of wave mechanics (to the same degree as the phenomenon of diffraction of electrons, atoms, or molecules, for example). Nonetheless, they can be used for an impressive demonstration of the quantum nature of ‘particles’. Indeed, suppose that one can throw very slow particles in the direction parallel to an impenetrable surface. Eventually, some part of energy of quantum fluctuations related to the transverse degree of freedom will be transformed into the energy of the motion of the center of the packet in the direction perpendicular to the boundary. Consequently, the particles will be *deflected from the boundary*.

In order to see a significant deflection, the initial mean velocity in the direction parallel to the surface, v_{\parallel} , must be of the same order of magnitude as the asymptotical transverse velocity given by Eq. (27): $v_{\infty} \approx \hbar/(2ms)$, where s is the initial width of the region of localization of the particle in the transverse direction (perpendicular to the boundary). Taking $s = 10^{-6}$ cm, we obtain $v_{\infty} \sim 5 \times 10^3$ m/s for electrons and $v_{\infty} \sim 2$ m/s for neutrons or hydrogen atoms, which correspond to the kinetic energies of the order of 10^{-4} eV and 10^{-8} eV, respectively.

Let us take the initial distance from the boundary $x_c = 1$ cm, which is a quite macroscopic parameter

(in this case $\beta \sim 10^6$). Then the particle will be deflected to the angle about 45° after the time interval

$$t_d \approx 5\beta/b^2 = 5\beta(ms^2/\hbar) \approx 4msx_c/\hbar \quad (32)$$

which equals $t_d^{(e)} \sim 5 \times 10^{-6}$ s for electrons and $t_d^{(n)} \sim 10^{-2}$ s for neutrons or hydrogen atoms. During this time the particle will pass about $2x_c$ in the parallel direction and about x_c in the perpendicular direction. So, the ‘quantum deflection’ can be quite observable, especially if one takes the initial distance x_c bigger, say, 10 cm. The effect is rather impressive from the classical point of view: a particle passes in 10 cm from the wall, nonetheless, in the absence of any visible force, it ‘feels’ the presence of the boundary and changes the direction of motion by 45° (or even more, if the initial parallel velocity is less than v_{∞}). In a wide sense, this is an analogue of the famous Aharonov–Bohm effect, when a charged particle is deflected by the localized magnetic flux, although it travels through the region where there is no magnetic field. Both phenomena have the same origin: quantum nonlocality and the existence of ‘wave properties’ of quantum objects.

However, to observe the effect of ‘quantum deflection’ one has to resolve several problems: to slow down the particles to the necessary velocity, to direct them in the proper direction with very small uncertainty in the transverse position, to compensate various external perturbations, and, finally, to detect the deflected particle. In the case of electrons, ‘cooling’ them to the energy about 10^{-4} eV ~ 1 K can be a difficult problem. Besides, although the gravitational force can be neglected due to the small mass, and the force of the electrostatic interaction with the surface (the attraction by the effective image charge) is also negligible due to the macroscopic distance, it could be rather difficult to ensure the variations of the electrostatic potential at the level less than 10^{-5} V in the region with dimensions of several centimeters.

The experiments with ultracold neutrons having velocities about 1 m/s have been performed for a long time [13,14]. It is unclear, however, how to prepare them in the necessary initial state. Therefore, the most promising candidates are ultracold atoms, since the methods of cooling them to the energies much below 10^{-8} eV $\sim 10^{-4}$ K are well elaborated,

and many experiments with such atoms have been done already [33–36]. Cooling atoms in a trap and letting them to exit the trap through some long thin ‘atom waveguide’ [37–39], one could prepare the necessary initial state with the velocity directed along the surface and with a small uncertainty in the transverse position.

In this case, the influence of gravity becomes essential, since the vertical shift of the hydrogen atom by 1 cm changes its potential energy by 10^{-9} eV. One can partially overcome this difficulty, using the *vertical* boundary and directing the particle upwards (some kind of the ‘atom fountain’ [40]). Moreover, adjusting the initial velocity, one can achieve zero displacement in the vertical direction due to the force of gravity, and a significant displacement in the horizontal direction due to the ‘quantum repulsive force’. For example, for the atoms of ^9Be and the initial distance $x_c \approx 3$ cm, one has $t_d \sim 0.3$ s. Taking the initial vertical velocity $v_{\parallel} \approx 1.5$ m/s, in 0.3 s one shall discover the neutral atom at the same horizontal level, but shifted (in average) to about 3 cm from the initial position, so that the center of the distribution will be in 6 cm from the boundary (the maximal vertical displacement will be about 10 cm). The same result holds for the hydrogen atoms, if the initial transverse position uncertainty is $s = 0.1 \mu\text{m}$. Unfortunately, increasing parameter s diminishes the asymptotical transverse mean velocity and increases the time t_d , which makes difficult the compensation of the gravity force. To verify the effect, one could put a detector at different positions at the same horizontal level and measure the probability of detecting the particles as a function of the distance to the boundary. The theoretical curve (Fig. 2) exhibits a strong asymmetry with respect to the initial particle position x_c . Moreover, if the space resolution of the detector could be made less than the initial transverse position uncertainty s , than the oscillations of the probability density due to the quantum interference effects could be discovered.

Note that the effect discussed does not depend on the internal state of the atom, since it is related only to the translational motion of its center of mass. Moreover, for the velocities required, the De Broglie wavelength has the same order of magnitude as the initial transverse uncertainty s , so it is much greater than the interatomic distances in solids. Therefore

the atomic structure of the solid surface seems to be unessential (since there is no ‘direct’ collision between the atom involved and the atoms of the boundary), and the surface seems to be close to an ideal impenetrable boundary. If it is not ideal for some reasons, one could use, e.g., the evanescent wave atomic mirrors [41–44], or magnetic mirrors [45,46]. In any case, in spite of many difficulties (we did not discuss, e.g., the problem of detecting the atoms), an experiment on ‘quantum deflection’ of ultracold atoms seems to be possible, and it could be interesting to try to do it.

Another conclusion is as follows. We have shown that in the presence of the wall, the mean momentum of a particle is changed at the expense of the energy of internal quantum fluctuations, due to some effective nonlocal quantum interaction. But the ideal wall is the limiting case of repulsive potentials. Therefore one could suppose that the initial form of the wave packet could be important in the processes of collisions between ultracold particles, when absolute values of their initial mean momenta are less or comparable with the square roots of the momenta dispersions (this is a further step to the true quantum domain, compared with the cases studied till now [47]). As a result of a distortion of the shapes of the particle wave packets during the collision, the absolute values of the *mean momenta* will not be conserved. In this sense, the collisions between ultracold particles turn out inelastic, as far as the initial states are not idealized plane waves, but wave packets of finite spatial extensions.

Acknowledgements

The authors thank Prof. S.S. Mizrahi for the fruitful discussions. MAA acknowledges the support of the Brazilian agency CNPq.

References

- [1] V.V. Dodonov, V.I. Man’ko, Invariants and the Evolution of Nonstationary Quantum Systems. in: M.A. Markov (Ed.), Proc. of Lebedev Physics Institute, vol. 183, Nova Science, Commack, 1989.

- [2] E. Heller, *J. Chem. Phys.* 62 (1975) 1544.
- [3] M. Andrews, *J. Phys. A* 14 (1981) 1123.
- [4] R.E. Turner, R.F. Snider, *Can. J. Phys.* 59 (1981) 457.
- [5] R.G. Littlejohn, *Phys. Rep.* 138 (1986) 193.
- [6] V.V. Dodonov, V.I. Man'ko, D.L. Ossipov, *Physica A* 168 (1990) 1055.
- [7] V.G. Bagrov, V.V. Belov, A.Yu. Trifonov, *Ann. Phys. (NY)* 246 (1996) 231.
- [8] T.E. Clark, R. Menikoff, D.H. Sharp, *Phys. Rev. D* 22 (1980) 3012.
- [9] L.S. Schulman, *Phys. Rev. Lett.* 49 (1982) 599.
- [10] E.A. Akhundova, V.V. Dodonov, V.I. Man'ko, *J. Phys. A* 18 (1985) 467.
- [11] B.K. Cheng, *J. Phys. A* 23 (1990) 5807.
- [12] V.V. Dodonov, A.B. Klimov, V.I. Man'ko, *Nuovo Cim. B* 106 (1991) 1417.
- [13] V.P. Alfimenkov, V.E. Varlamov, A.V. Vasil'eV et al., *JETP Lett.* 52 (1990) 373.
- [14] V.K. Ignatovich, *Uspekhi Fiz. Nauk* 166 (1996) 303 [*Physics - Uspekhi* 39 (1996) 283].
- [15] H. Wallis, J. Dalibard, C. Cohen-Tannoudji, *Appl. Phys. B* 54 (1992) 407.
- [16] C.G. Aminoff, A.M. Steane, P. Bouyer, P. Desbiolles, J. Dalibard, C. Cohen-Tannoudji, *Phys. Rev. Lett.* 71 (1993) 3083.
- [17] P. Szriftgiser, D. Guéry-Odelin, M. Arndt, J. Dalibard, *Phys. Rev. Lett.* 77 (1996) 4.
- [18] J.P. Dowling, J. Gea-Banacloche, *Adv. At. Mol. Opt. Phys.* 37 (1996) 1.
- [19] J. Gea-Banacloche, *Am. J. Phys.* 67 (1999) 776.
- [20] M.A. Doncheski, R.W. Robinett, *Eur. J. Phys.* 20 (1999) 29.
- [21] M. Andrews, *Am. J. Phys.* 66 (1998) 252.
- [22] I.A. Malkin, V.I. Man'ko, D.A. Trifonov, *Phys. Rev. D* 2 (1970) 1371.
- [23] V.V. Dodonov, V.I. Man'ko, *Phys. Rev. A* 20 (1979) 550.
- [24] V.V. Dodonov, I.A. Malkin, V.I. Man'ko, *Physica* 72 (1974) 597.
- [25] V.V. Dodonov, E.V. Kurmyshev, V.I. Man'ko, *Phys. Lett. A* 79 (1980) 150.
- [26] H.P. Yuen, *Phys. Rev. Lett.* 51 (1983) 719.
- [27] P. Storey, T. Sleator, M. Collett, D. Walls, *Phys. Rev. A* 49 (1994) 2322.
- [28] D. Walls, *Austral. J. Phys.* 49 (1996) 715.
- [29] E. Heller, in: M.-J. Giannoni, A. Voros, J. Zinn-Justin (Eds.), *Chaos and Quantum Physics*, Elsevier, Amsterdam, 1991, p. 547.
- [30] V.V. Dodonov, V.I. Man'ko, in: M. Evans, S. Kielich (Eds.), *Modern Nonlinear Optics, Advances in Chem. Phys. Series*, vol. LXXXV, Wiley, New York, 1994, Part 3, p. 499.
- [31] R.A. Campos, *J. Mod. Opt.* 46 (1999) 1277.
- [32] A. Erdélyi (Ed.), *Bateman Manuscript Project: Higher Transcendental Functions*, vol. II, McGraw-Hill, New York, 1953.
- [33] J. Mlynek, V. Balykin, P. Meystre (Eds.), *Optics and Interferometry with Atoms*, special issue of *Appl. Phys. B* 54 (1993) 319.
- [34] H. Metcalf, P. van der Straten, *Phys. Rep.* 244 (1994) 204.
- [35] K.G.H. Baldwin, *Austral. J. Phys.* 49 (1996) 855.
- [36] C.N. Cohen-Tannoudji, *Rev. Mod. Phys.* 70 (1998) 707.
- [37] M.J. Renn, D. Montgomery, O. Vdovin, D.Z. Anderson, G.E. Wieman, E.A. Cornell, *Phys. Rev. Lett.* 75 (1995) 3253.
- [38] M.V. Subbotin, V.I. Balykin, D.V. Laryushin, V.S. Letokhov, *Opt. Commun.* 139 (1997) 107.
- [39] V.I. Balykin, *Adv. At. Mol. Opt. Phys.* 41 (1999) 181.
- [40] M.A. Kasevich, E. Riis, S. Chu, R.G. De Voe, *Phys. Rev. Lett.* 63 (1990) 612.
- [41] R. Cook, R. Hill, *Opt. Commun.* 43 (1982) 258.
- [42] V.I. Balykin, V.S. Letokhov, Y.B. Ovchinnikov, A.I. Sidorov, *Phys. Rev. Lett.* 60 (1988) 2137.
- [43] M.A. Kasevich, D.S. Weiss, S. Chu, *Opt. Lett.* 15 (1990) 607.
- [44] R. Grimm, M. Weidemuller, Y.B. Ovchinnikov, *Adv. At. Mol. Opt. Phys.* 42 (2000) 95.
- [45] K.S. Johnson, M. Drndić, J.H. Thywissen, G. Zabow, R.M. Westervelt, M. Prentiss, *Phys. Rev. Lett.* 81 (1998) 1137.
- [46] E.A. Hinds, I.G. Hughes, *J. Phys. D: Appl. Phys.* 32 (1999) R119.
- [47] J. Weiner, V.S. Bagnato, S. Zilio, P.S. Julienne, *Rev. Mod. Phys.* 71 (1999) 1.